

# SIMULATION STUDY ON ECI FOR BEPC AND BEPCII\*

J. Xing, Z.Y. Guo, Q. Qin, J.Q. Wang

Institute of High Energy Physics, Chinese Academy of Sciences, Beijing, 100039, P.R. China

## INTRODUCTION

The Beijing Electron Positron Collider will be upgraded to enhance the luminosity in the energy of 1.89 GeV. The machine will become a double ring (BEPCII) from a single ring. The multi-bunch electron and positron beams will circle in each ring respectively. The electron cloud instability is suspected to occur in the positron ring, and it may influence the luminosity performance of the collider. A simulation code has been developed based on similar programs, which have been used to study ECI in other laboratories. The physics model of the instability, the simulation results comparing to the observation in the BEPC experiments and simulation results on the BEPCII design study will be discussed in this paper.

## PART I REVIEW OF EXPERIMENT AND SIMULATION STUDY ON BEPC

### 1. Instrumentation 1.1 PE detector

Similar to the detector in the APS[2,3], a photoelectron detector was installed in the BEPC ring. It has three layers with the same diameter of 80 mm and two mesh grids in front of the detector. The outermost grid is grounded, and a bias voltage is applied to the shielded grid. The graphite-coated collector lowers the secondary electron yield and is biased with a DC voltage of +48 V with batteries. Between the detector and the support barrel mounted on an idle slot, a 1 cm annular gap exists.

The detector is mounted downstream of a dipole in the direction of positron motion, shown in Fig. 1.

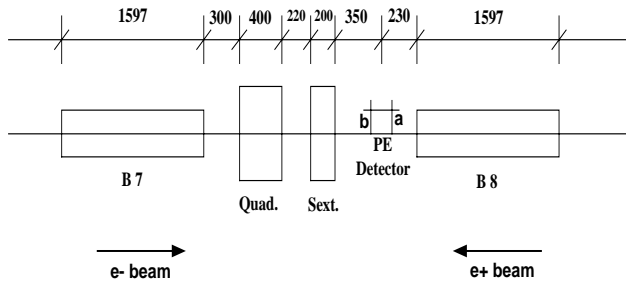


Figure 1: Position of the PE detector at the BEPC storage ring (seen from inside of the ring).

Being so close to the dipole, the PE detector has to be shielded from the magnetic field with layers of high and low permeability “mu-metal” sheets and nickel alloy sheets. After shielding, the fields at the points *a* and *b* in Fig. 1 are 9 Gauss and 0, respectively.

### 1.2 Apparatus setup

The detector is connected with other instruments as shown in Fig. 2. A low pass filter (LPF) is used to make sure that the signal of collector is from the electron only. The current of photoelectron is measured with the nanoampere-meter, which is connected between the resistor and ground. A temperature monitor is mounted on the detector to detect heat induced by beam-excited HOM wakefields in the annular gap between the detector and the support barrel.

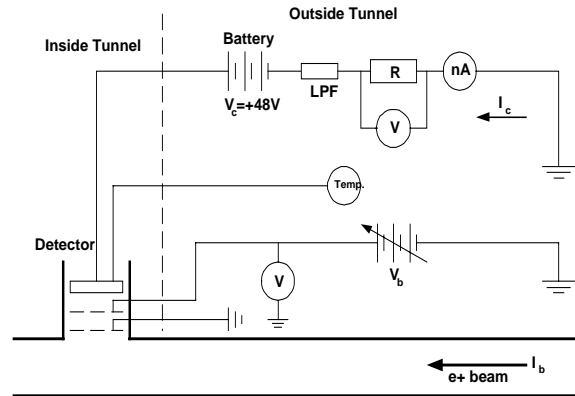


Figure 2: Setup of all apparatus in the experiment.

## 2 Measurements

In the following PE measurements, we apply the 150 MHz LPF to eliminate any sources of RF noise. During all the measurement, the temperature monitor displays  $24 \pm 1^\circ\text{C}$  with no change, which means the HOMs effect due to the annular gap between the detector and its support barrel is minimal. A bias voltage scan was made and the  $V_b$  fixed at +40V for maximum signal, as shown in Fig. 3. The derivative of the normalized  $I_c - V_b$  curve gives the photoelectron energy distribution, shown as Fig. 4.

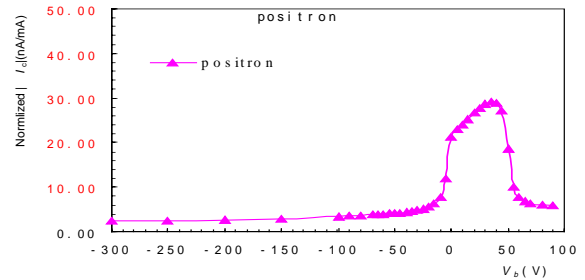


Figure 3: Detector current during bias voltage scan.

\*Work supported by the Chinese National Foundation of Natural Sciences, contracts 19875063-A050501 and 19975056-A050501

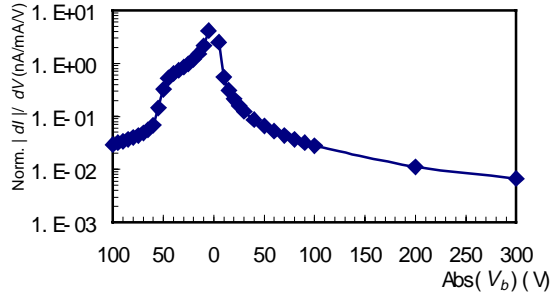


Figure 4: Photoelectron energy distribution.

### 2.1 Dependence on beam current

The collected electron current  $I_c$  as a function of beam current  $I_b$  is measured in the cases of single bunch and multi-bunch. Normalized by  $I_b$ ,  $I_c$  is almost the same in different bunch spacing. It reads about 25nA/mA at the bunch current of 2 mA, similar to the plot in Fig. 5.

No saturation effect, in which electron generation and loss equilibrate, is found with a long bunch train and a weak bunch current, even if 40 bunches are used with the bunch current of 1 or 2 mA ( $I_b$  is 40 or 80 mA).

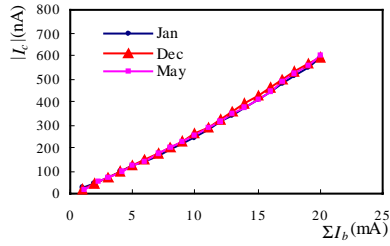


Figure 5: Collected electron current  $I_c$  as a function of beam current  $I_b$

### 2.2 Secondary electron (SE) measurement

Due to the SE, a dramatic amplification of the signal is observed in the APS when the bunch spacing is 7 buckets (20 ns) [2]. But in our measurements, such an amplification is not observed as shown in Fig. 6.

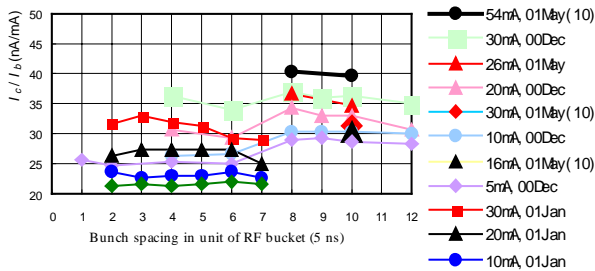


Figure 6: Normalized electron current as a function of bunch spacing and current. The legend gives beam current.

### 2.3 Solenoid effect

Solenoid coils winding downstream of the dipoles is a possible way to cure the PEI, like KEKB LER. In BEPC storage ring, we installed two coils on each side of the detector to observe the solenoid effect. The currents of the coils,  $I_s$ , are  $\pm 20$ A, generating several tens of Gauss magnetic field. Fig. 7 shows the  $I_c$  vs.  $I_b$  when solenoid has different currents.

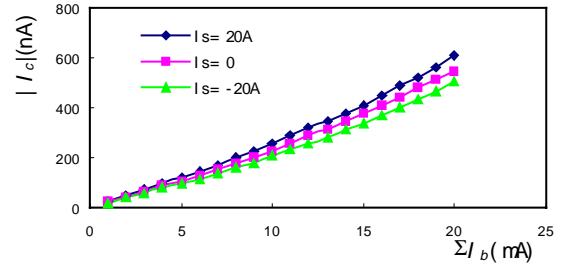


Figure 7:  $I_c$  vs.  $I_b$  with different solenoid fields.

## 3 Simulations

With the code developed by Dr. Y. Luo [4], the PE generation is simulated for different PE reflectivity. For a real machine, a reflectivity of 0.98 is chosen in simulation. The energy distribution of the PE is selected as  $5\text{eV} \pm 5\text{eV}$ . The emission yield of secondary electron is given as

$$\delta(E, \theta) = \delta_{\max} \cdot 1.11 \cdot \left( \frac{E}{E_{\max}} \right)^{-0.35} \cdot \left( 1 - \exp \left[ -23 \cdot \left( \frac{E}{E_{\max}} \right)^{1.35} \right] \right) / \cos \theta$$

with  $\cos \theta$  distribution as the angle distribution. The energy distribution of the SE is  $0 \pm 5\text{eV}$ , and the  $\delta_{\max}$  of the SE is 3 in simulation. Simulation results are shown in Fig. 8 and 9.

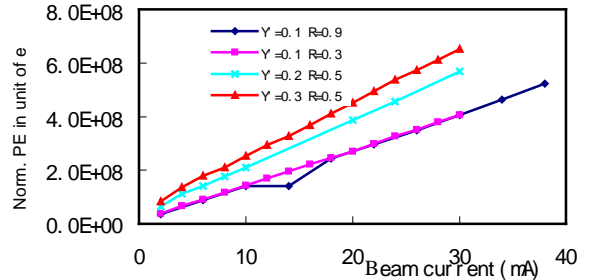


Figure 8: PE creation for different yield and reflectivity.

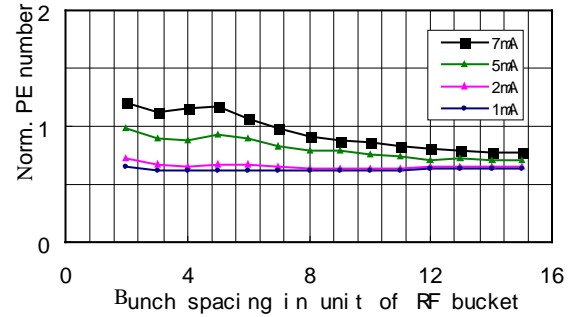


Figure 9: Simulation results on multipacting. (The legend gives bunch current.)

## 4 Discussions

Detailed measurements of the properties of PE cloud were carried out at the BEPC storage ring under various beam conditions.  $I_c$  varies linearly with the beam current  $I_b$  as expected. No saturation process is observed up to 40 bunches with 1 or 2 mA/bunch. We observed very weak dependence on bunch spacing, using 5 and 10 bunches

with 1 to 6 mA/bunch up to the 12-bucket spacing. No beam-induced multipacting was observed at the BEPC yet.

Two new detectors, modified as encircling the grounded grid but isolated from the retarding grid and the collector to avoid the  $I_c$  electrical leak from HOMs excited through the gap between the detector and the port, will be installed soon in the places far from dipoles. The time structure of  $I_c$  signal and the machine parameter dependences would be studied furthermore. Better shielding is necessary on the existing detector to avoid the fringe field of the dipole.

Primary simulations give some consistent results with the experiments, especially the multipacting condition and the dependences of beam parameters. More simulation studies are still under way.

## PART II SIMULATION STUDY ON BEPCII

BEPCII is an upgrade project of Beijing electron-positron collider(BEPC), which will install a new inner ring based on the single-ring collider BEPC. It will provide the colliding beams of the center-mass between 1.0 GeV and 2.0 GeV and also the dedicated synchrotron radiation beam at 2.5 GeV. For the colliding beams the luminosity is optimized at 1.89 GeV with  $10^{33}$  cm<sup>-2</sup>s<sup>-1</sup>, which is two order of magnitude of BEPC. Some parameters of BEPCII is compared with that of some other machines in table 1 [5].

Table 1: Parameters of a few storage rings

	BEPCII	KEKB	PEPII
Beam energy(GeV)	1.89	3.5	3.1
Bunch population $N_b(10^{10})$	4.84	3.3	9
Bunch spacing $L_{sep}(m)$	2.4	2.4	2.5
Rms bunch length $s_b(m)$	0.015	0.004	0.013
Rms bunch sizes $s_{x,y}(mm)$	1.18,0.15	0.42,0.06	1.4,0.2
Chamber half dimensions $h_{x,y}(mm)$	60,27	47	25
Slippage factor $h(10^{-3})$	22	0.18	1.3
Synchrotron tune $Q_s$	0.033	0.015	0.03
Circumference C(km)	0.24	3.0	2.2
Average beta function(m)	10	15	18
Parameter $n_{min}$	9.24	10	1
e- oscillation/bunch $n_{osc} w^0 s_z/(pc)$	0.42	1.0	0.9
Density enhancement $H_c$	15	13	12
Adiabaticity $A$	17.4	9	8
TMCI threshold $r_c[10^{-12}m^{-3}]$	22.7	0.5	1
Density ratio $r_{csat}/r_{c,threshold}$	0.19	4	4

**1. Electron cloud Build up and Saturation** The ECLoud programme developed by O. Bruning, G. Rumolo, F. Zimmermann of the CERN SL Division was used in the simulation study on the build up and saturation of the electron cloud on BEPCII. [6]

### 1.1 the photo-emission yield and the SEY

For BEPCII, The number of radiated photons per positron is about 12 photons for one dipole bending magnet. And From figure 10. , the “first strike” photons in the dipole magnet region is approximately equal to that in

the field free region. And consider the effect of the antichamber, only ~1% of the radiated photons can remain inside the chamber[7][8]. Assume the electron yield per absorbed photon is 0.1, then the photonelectron yield  $Y_{pe}$  will be 0.006. Simulation result also shows that coating the inner face of the vacuum chamber with TiN will effectively reduce the number of the electrons, as shown in Fig. 11 [7].

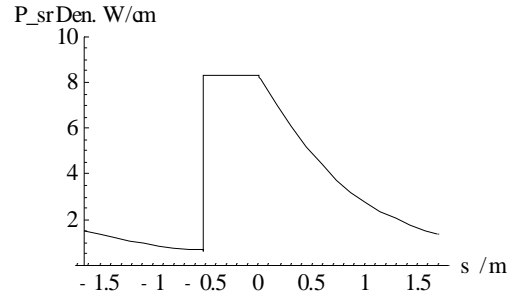


Figure10: SR power distribution along the ring(-1.6 < s < 0, means in the dipole magnet region)

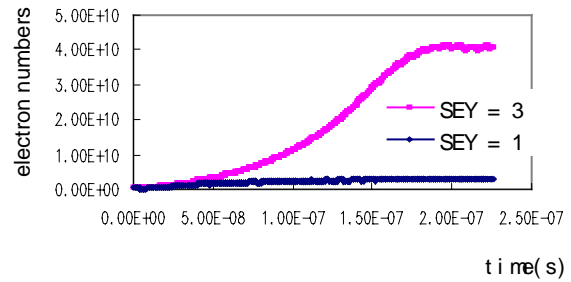


Figure 11: Electron numbers with and without TiN coating of the chamber.( $Y_{e,ph}=0.006$ )

### 1.2 The electron cloud build up and saturation

The build up and saturation of electron cloud under different conditions and possible cures were simulated, as shown in Fig.12, Fig.13, Fig. 14 and Fig.15.[9] The dipole magnets which will occupy about 25% of the whole ring, will confine many electrons to the vicinity of the pipe wall. Thus the volume density of the electrons will be reduced.[5]

The effect of the solenoid and the clearing electrode that had been successfully used to suppress the ECI were also studied for BEPCII.

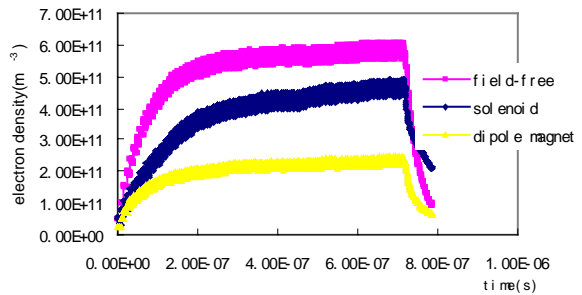


Figure 12: the average electron density of the pipe per cubic meter in the dipole magnet compared with that in the free field region with and without solenoid.

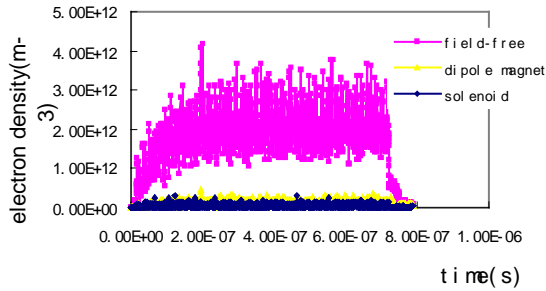


Figure 13: Electron density at the center of the pipe per cubic meter in the dipole magnet compared with that in the free field region with and without solenoid.

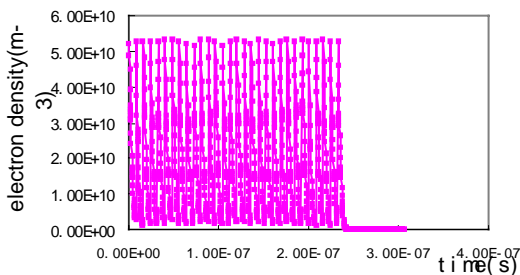
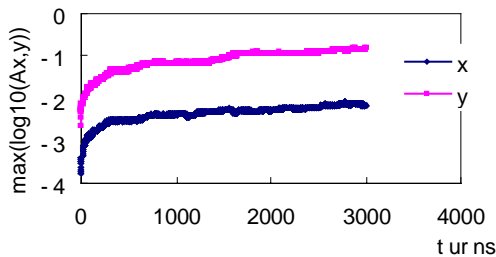


Figure 14: The average electron density of the pipe per cubic meter for a field-free region with clearing electrode (500V) vs. time.

## 2. Electron cloud instabilities

### 2.1 The coupled-bunch instability

The “turn by turn” code developed by Dr. Y. Luo was used. The rise time got from figure15 is about 0.3ms.



[4] Figure.15:  $\max(\log_{10}(A_{x,y}))$  vs turns

### 2.2 the single-bunch instability

The **headtail** programme developed by G. RUMOLO was used in the simulation study. [6][9]

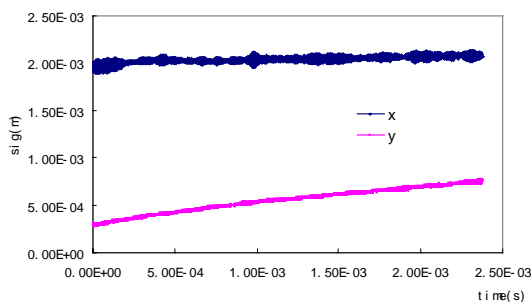


Figure 16: Sqrt(beam size) growth as a function of time in the field-free Region, assuming that the electron density is  $2.0 \times 10^{12}/m^3$ .

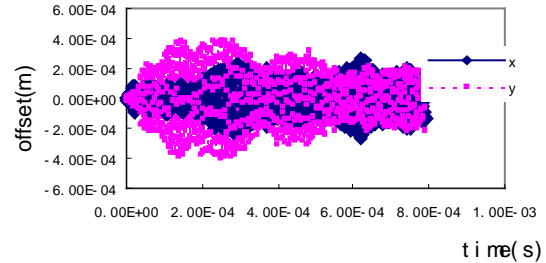


Figure 17: Simulated beam centroid motion as a function of time in the field-free region ,assume the elcetron density is  $2.0 \times 10^{12}/m^3$ .

## 3 Discussions

The preliminary result shows that the instabilities caused by the ecloud will not be very serious. The very important condition is that the BEPCII will run below the TMCI threshold of the ecloud. Also it will benefit from the strong dipole magnet and other cures.

More details which will be closer to the actual conditions will be studied in the future.

## ACKNOWLEDGEMENTS

We wish to thank the BEPC team for their effective work on operating the machine during the experiment. The authors would also like to thank R. Rosenberg from ANL, for his suggestion on shielding the detector.

The authors would also like to thank F. Zimmermann, G. Rumolo, K. Ohmi, L. Wang and H. Fukuma for their support.

## REFERENCES

- [1] Z.Y. Guo, et al, Proc. of PAC'97, 1997, EPAC'98, APAC'98, 1998.
- [2] K. Harkay, R. Rosenberg, Proc. of PAC'99, 1999.
- [3] R. Rosenberg, K. Harkay, NIM A 453 (2000) 507.
- [4] Y. Luo, IHEP Ph.D dissertation, 2000.
- [5] F. Zimmermann, PAC 2001, CERN-SL-2001-0035.
- [6] F. Zimmermann, Chamonix X & XI, CERN-SL-2000-007 & 2001-003-DI; G. Rumolo et al., PRST-AB 012801(2001).
- [7] M. A. Furman, G. R. Lamberson, PEP-II AP Note AP 97.27.
- [8] J. Wang, BEPCII-AP-Note/2001-06.
- [9] G. Rumolo, F. Zimmermann, CERN-SL-2001-041.